



# Hepatic encephalopathy is linked to alterations of autophagic flux in astrocytes

Kaihui Lu<sup>a,#</sup>, Marcel Zimmermann<sup>a,#</sup>, Boris Görg<sup>b</sup>, Hans-Jürgen Bidmon<sup>c</sup>,  
 Barbara Biermann<sup>d</sup>, Nikolaj Klöcker<sup>d</sup>, Dieter Häussinger<sup>b</sup>, Andreas S. Reichert<sup>a,\*</sup>

<sup>a</sup> Institute of Biochemistry and Molecular Biology I, Heinrich Heine University Düsseldorf, Medical Faculty, Düsseldorf, Germany

<sup>b</sup> Department of Gastroenterology, Hepatology and Infectious Diseases, Heinrich Heine University Düsseldorf, Medical Faculty, Düsseldorf, Germany

<sup>c</sup> C. & O. Vogt Institute for Brain Research, Heinrich Heine University Düsseldorf, Medical Faculty, Düsseldorf, Germany

<sup>d</sup> Institute of Neural and Sensory Physiology, Heinrich Heine University Düsseldorf, Medical Faculty, Düsseldorf, Germany

## ARTICLE INFO

### Article history:

Received 13 March 2019

Revised 18 September 2019

Accepted 19 September 2019

Available online 21 October 2019

### Keywords:

Hepatic encephalopathy

Liver disease

Autophagy

Lysosome

Taurine

## ABSTRACT

**Background:** Hepatic encephalopathy (HE) is a severe neuropsychiatric syndrome caused by various types of liver failure resulting in hyperammonemia-induced dysfunction of astrocytes. It is unclear whether autophagy, an important pro-survival pathway, is altered in the brains of ammonia-intoxicated animals as well as in HE patients.

**Methods:** Using primary rat astrocytes, a co-culture model of primary mouse astrocytes and neurons, an *in vivo* rat HE model, and *post mortem* brain samples of liver cirrhosis patients with HE we analyzed whether and how hyperammonemia modulates autophagy.

**Findings:** We show that autophagic flux is efficiently inhibited after administration of ammonia in astrocytes. This occurs in a fast, reversible, time-, dose-, and ROS-dependent manner and is mediated by ammonia-induced changes in intralysosomal pH. Autophagic flux is also strongly inhibited in the cerebral cortex of rats after acute ammonium intoxication corroborating our results using an *in vivo* rat HE model. Transglutaminase 2 (TGM2), a factor promoting autophagy, is upregulated in astrocytes of *in vitro*- and *in vivo*-HE models as well as in *post mortem* brain samples of liver cirrhosis patients with HE, but not in patients without HE. LC3, a commonly used autophagy marker, is significantly increased in the brain of HE patients. Ammonia also modulated autophagy moderately in neuronal cells. We show that taurine, known to ameliorate several parameters caused by hyperammonemia in patients suffering from liver failure, is highly potent in reducing ammonia-induced impairment of autophagic flux. This protective effect of taurine is apparently not linked to inhibition of mTOR signaling but rather to reducing ammonia-induced ROS formation.

**Interpretation:** Our data support a model in which autophagy aims to counteract ammonia-induced toxicity, yet, as acidification of lysosomes is impaired, possible protective effects thereof, are hampered. We propose that modulating autophagy in astrocytes and/or neurons, e.g. by taurine, represents a novel strategy to treat liver diseases associated with HE.

**Funding:** Supported by the DFG, CRC974 “Communication and Systems Relevance in Liver Injury and Regeneration”, Düsseldorf (Project number 190586431) Projects A05 (DH), B04 (BG), B05 (NK), and B09 (ASR).

© 2019 The Author(s). Published by Elsevier B.V.

This is an open access article under the CC BY-NC-ND license.

(<http://creativecommons.org/licenses/by-nc-nd/4.0/>)

**Abbreviations:** CCCP, carbonyl cyanide m-chlorophenylhydrazone; CQ, chloroquine; EM, electron microscopy; HE, hepatic encephalopathy; IF, Immunofluorescence; LC3, microtubule-associated protein 1A/1B-light chain 3; mQC, mitochondrial quality control; MSO, L-methionine-S-sulfoximine; NAC, N-acetyl-L-cysteine; Rapa, rapamycin; ROS, reactive oxygen species; TGM2, transglutaminase 2; WB, Western Blot.

\* Corresponding author.

E-mail address: [reichert@hhu.de](mailto:reichert@hhu.de) (A.S. Reichert).

# These two authors contributed equally

<https://doi.org/10.1016/j.ebiom.2019.09.058>

2352–3964/© 2019 The Author(s). Published by Elsevier B.V. This is an open access article under the CC BY-NC-ND license.

(<http://creativecommons.org/licenses/by-nc-nd/4.0/>)

## Research in Context

### Evidence before this study

Liver failure, as for example caused by excessive alcohol abuse or liver cancer, very frequently results in cognitive impairments and can lead to coma and death. The current view on the pathogenesis of this severe neuropsychiatric syndrome, termed hepatic encephalopathy (HE), is an underlying failure to detoxify excess of ammonia originating largely from gut-resident bacteria. Ammonia levels subsequently increase in the blood and the cerebral fluid causing primarily toxic effects to astrocytes. This toxicity is largely attributed to increased osmotic swelling and oxidative stress, which promotes protein and nucleic acid modifications, subsequently alters gene expression, and impairs brain functionality. Protective mechanisms aiming to counteract ammonia-induced toxicity are not well understood. Autophagy is a well-known pro-survival pathway ensuring the efficient removal of damaged molecules or organelles and impairment thereof is strongly linked to cancer (e.g. liver cancer) and numerous neurodegenerative diseases. Albeit ammonia is known to impair autophagy in numerous cell types including cancer cells and liver cells, it was unclear whether autophagy is altered under conditions of hyperammonemia in astrocytes, in neurons, in animal HE models, or in the brain of patients suffering from HE. Prior to this study it was also not known whether modulation of autophagy in astrocytes could represent a therapeutic strategy for treating HE.

### Added value of this study

We provide several lines of evidence that autophagy is modulated in astrocytes, in neurons, in brain tissue derived from an animal HE model and from liver cirrhosis patients suffering from HE. We gained a detailed mechanistic picture on ammonia-induced toxicity on autophagy which was shown to depend on impaired acidification of lysosomes and formation of reactive oxygen species. Our data point to an updated view on the pathogenesis of HE suggesting that impaired autophagy in the brain is a novel critical factor. We further show that taurine, a compound known to have beneficial effects in the context of neurodegenerative and liver diseases, improves autophagic flux in astrocytes and in brain tissue from an animal HE model under hyperammonemia. Taurine does not appear to act via inhibiting the classical mTOR signalling pathway to induce autophagy but alleviates ammonia-induced ROS formation.

### Implications of all the available evidence

Our study opens a novel, expanded view on the pathogenesis of HE suggesting that impaired autophagy, an important cellular quality control mechanisms, has to be considered in future studies. We propose that improving autophagy in particular in astrocytes, as exemplified by the use of taurine, represents a novel strategy for treating HE.

## 1. Introduction

Hepatic encephalopathy (HE) is a quite common and severe neuropsychiatric syndrome caused by liver failure and subsequent hyperammonaemia [1],[2]. HE is characterized by low grade cerebral edema and increased cerebral oxidative/nitrosative stress. 30 to 80% of all patients suffering from liver cirrhosis develop neurocognitive deficits that are classified as HE or as the earliest stage of HE, minimal HE [3]. Astrocytes are critical for the detoxification of ammonia in the brain and impairment of astrocyte function is well accepted to be the primary cause for subsequent neu-

ronal damage and ultimate cognitive and motoric symptoms [1]. Though numerous studies tried to elucidate the molecular mechanism behind the development of the disease, a comprehensive picture is still missing. Ammonia is for example discussed to alter glutamate/glutamine metabolism [4],[5]. Such a metabolic imbalance is regarded as a possible cause for the generation of reactive oxygen species (ROS) and reactive nitrogen species (RNS), which are key factors for downstream observed RNA oxidation, tyrosine nitration and other oxidative damages in the development of HE [6–8]. Other studies observed additional biological consequences in different HE models including impaired mitochondrial functions [9],[10], altered signal transduction [11], post-translational modifications [12], senescence and changes in microRNA expression [13].

Cytosolic material is degraded via autophagy which is known to eliminate toxic components and to provide nutrients under various stress conditions [14]. Autophagy is critical for a wide range of cellular processes such as cellular homeostasis, cancer, aging, developmental processes, and programmed cell death type II [15]. Autophagy is known to act in a protective manner in various neurodegenerative diseases and to counteract (1) the progression from steatosis to non-alcoholic steatohepatitis (NASH), (2) ammonia-induced toxicity in acute and chronic animal models, (3) formation of hepatocellular carcinomas (HCCs), and (4) toxin-induced liver dysfunction [16–19]. Furthermore, using several animal models it was shown that hyperammonemia results in altered muscle autophagy contributing to loss of skeletal muscle (sarcopenia) [20].

Given the importance of autophagy as a protective mechanism against various forms of external stresses including ROS and the known fact that ammonia impairs autophagy in fibroblasts and tumor cells [21],[22], we decided to test whether autophagy is possibly also modulated in astrocytes and/or the brain upon hyperammonemia. Here we provide several lines of evidence (using *in vitro*, *in vivo*-HE models, as well as HE patient data) suggesting that impaired autophagy is critical for the pathogenesis of HE. We further show that taurine, a compound known to have beneficial effects in the context of liver diseases, improves autophagic flux despite the presence of high concentrations of ammonia. We propose that improving autophagy in astrocytes and/or neurons represents a novel strategy for treating HE in the future.

## 2. Materials and methods

### 2.1. Cell lines, culture conditions, cell viability assays

Human embryonic kidney cells HEK293 and human adenocarcinoma cell line HeLa were from ATCC (Manassas, USA). Human hepatocyte carcinoma cell line HepG2 and human astrocytoma cell line MOG-G-CCM were from ECACC (Salisbury, UK) while human neuroblastoma cell line SH-SY5Y was from DSMZ (Braunschweig, Germany). For further details of reagents, material, cell viability assays, and cell culture conditions see supplement.

### 2.2. Preparation of primary rat astrocytes

All animal experimental protocols have been approved by Institutional Animal Care and Use Committee, Heinrich Heine University Düsseldorf. Primary rat astrocytes are prepared from the cerebral cortex of newborn Wistar rats as described previously [23].

### 2.3. Preparation of primary mouse neurons

Primary hippocampal neurons were prepared from embryonic C57BL/6J mice as described previously with minor modifications [24],[25]. Briefly, embryonic day 16 mouse hippocampi were dissected in Hank's balanced salt solution (1 × HBSS w/o Ca<sup>2+</sup> w/o Mg<sup>2+</sup> plus 10 mM HEPES), digested with 0.05% trypsin for 15 min

at 37 °C, dissociated by trituration, and plated on poly-D-lysine coated glass coverslips. Neurons were seeded at a density of 50,000 on 12 mm and 500,000 on 30 mm diameter coverslips and incubated in Neurobasal Medium plus 7.5% fetal bovine serum, 1% Na-Pyruvate, 1% Fungizone and 1% penicillin/streptomycin (P/S) at 37 °C / 5% CO<sub>2</sub> to allow attachment of neurons to the coverslips. After 3–4 h the medium was exchanged to glia-conditioned Neurobasal Medium enriched with 2% B27@Serum-free Supplement, 1% Na-Pyruvate, 1% Fungizone and 1% P/S by transferring the neuron-containing coverslips to culture dishes with astroglia feeder cells prepared from embryonic day 16 cortices from the same mice as above. To inhibit proliferation of astrocytes cytosin arabinoside (1-β-D-arabinofuranosylcytosine) was added to the culture medium after two days-in-vitro (DIV2) at a final concentration of 5 μM. After three weeks cells were subjected to treatments and analyses.

#### 2.4. In vivo rat HE model of acute ammonium intoxication

Hyperammonemia was induced in young adult male Wistar rats (weight 280 g ± 6 g) by intraperitoneal injection of ammonia acetate (4.5 mmol/kg body weight in 0.9% NaCl) [26]. Controls were treated with an equal amount of vehicle (0.9% NaCl) only. Taurine (5%) was given in drinking water for five consecutive days prior to ammonia acetate or the vehicle injection. 24 h after injection of ammonia acetate or vehicle, animals were deeply anesthetized, transcardially perfused with ice-cold physiological saline containing 5,000 I.E. heparin/L (Rotexmedica), and the cerebral cortex was dissected from blood free brain tissue.

#### 2.5. SDS-PAGE and western blot

Experimental procedures for all cell lines except neurons were done as described previously [27]. Neurons were washed twice with PBS, lysed with cold RIPA buffer (+ complete protease inhibitor, + phosphatase inhibitor cocktail 2) for 10 min, scraped in RIPA buffer and subsequently centrifuged for 20 min at 16,000 g. Densitometry was performed using non-saturated exposures for indicated number of independent experiments. For details such as antibodies see supplement.

#### 2.6. Fluorescence microscopy

Fluorescence microscopy was used to visualize the GFP-LC3 puncta. Cells were transfected with appropriate amounts (1 μg / 35 mm dish) of pEGFP-LC3 plasmid using Effectene transfection reagent according to the manufacturer's protocol. 24 h after transfection, cells were seeded onto MatTek dishes. 48 h after transfection, cells were treated as indicated. Imaging at different time points was done using the Axio observer D1 fluorescent microscopy (Carl Zeiss) with 63 × objective. ZEN 2012 software was used to prepare the images.

#### 2.7. LysoSensor™ fluorescence microscopy

Astrocytes were seeded in MatTek dishes 48 h before experiments. Cells were treated with 5 mM NH<sub>4</sub>Cl or water for 72 h. After treatment, cells were stained with 1 μM LysoSensor™ Green DND-189 (Invitrogen) for 30 min. For NH<sub>4</sub>Cl-treated group, 5 mM NH<sub>4</sub>Cl was present during the staining procedure. Astrocytes were then imaged with the same setting using the spinning disk confocal microscopy (Eclipse Ti microscope (Nikon) and UltraVIEW vox spinning disk confocal system (PerkinElmer)).

#### 2.8. Electron microscopy (EM) and immunofluorescence (IF)

Experimental procedures for EM and IF in astrocytes were done as previously described [27]. For IF of neurons, cells were fixed and immunostained as described previously [28], using rabbit anti-LC3 (1:250), chicken anti-MAP2 (1:10,000), goat anti-rabbit Abberior STAR 635P, and goat anti-chicken Alexa Fluor® 488. After staining, neurons were mounted using ProLong Diamond Antifade Mountant. Confocal images were taken on Leica TSC SP8 STED 3X using the 100 × /NA1.4 oil objective and the white-light-laser. The same laser configurations were used for all four probes and image processing was performed equally in each channel.

#### 2.9. CellROX fluorescence microscopy

MOG-G-CCM astrocytoma cells were seeded 24 h before treatment. Cells were treated with 5 mM taurine and/or 5 mM NH<sub>4</sub>Cl for 72 h (30 min taurine pretreatment). 2.5 μM CellROX™ green were added and incubated for 40 min. Cells were washed 3 times with PBS and DMEM medium was applied. Cells were immediately imaged in a temperature and CO<sub>2</sub>-controlled microscope chamber. The same settings were chosen for all images recorded.

#### 2.10. Image analysis

GFP-LC3 puncta in GFP-LC3 transfected cells and acidic lysosome puncta in LysoSensor™-stained cells were manually counted. For analysis of autophagosomal area per cell, cells were manually outlined, the same threshold value for LC3 fluorescence was chosen for all pictures, and the total area of LC3 signal above threshold was measured within a cell. The ratio of “LC3 cluster versus MAP2” was analyzed using FIJI by equally thresholding the LC3-images in one experiment and using the wand tracing tool to select and load identified above-threshold-clusters to the ROI-Manager for subsequent measurement of the overall cluster size per image. For MAP2, the total area above-threshold was determined per image. The total LC3 fluorescence of IHC slices was determined as the mean grey value of the whole picture. Brain sections of intoxicated rats were analyzed by immunofluorescence staining for LC3 using a Zeiss LSM880 microscope. Glutamin synthetase (GS) as glia cell marker or neuronal nuclei (NeuN) antigen were co-stained with LC3. LC3 intensity was determined from the total LC3 signal (‘raw integrated intensity’) relative to controls (without NH<sub>4</sub>Ac) which were set to 1. For CellROX quantification images were background corrected with a fixed value, cells were manually selected, and a fixed stack size of 20 μm of an area was analyzed for voxel intensity. The mean and sum intensity of this voxel volume was then again manually background corrected for each image individually. The sum of voxel intensity correlated with cell size, while the mean has a cell size-independent value.

#### 2.11. Cathepsin L activity assay

Cultured rat astrocytes were treated with 5 mM NH<sub>4</sub>Cl, CH<sub>3</sub>NH<sub>4</sub>Cl, or 1.5 mM H<sub>2</sub>O<sub>2</sub> as positive control. 72 h after NH<sub>4</sub>Cl/CH<sub>3</sub>NH<sub>3</sub>Cl treatment, cathepsin L activity was analyzed via Magic red cathepsin L assay kit (Immunochemistry technology), according to the manufacturer's manual (protocol 15). Red (592 nm excitation; 628 nm emission) fluorescence was detected by Microplate reader infinite 200 PRO (Tecan).

## 2.12. Post mortem human brain tissue and microarray analysis

Patient characteristics/histories and details of microarray analysis have been described previously [29]. TGM2 gene expression levels were taken from data sets acquired in two earlier studies using Agilent™ whole human genome microarray analysis [29],[30]. Microarray analysis was performed by Miltenyi-Biotec (Bergisch Gladbach, Germany). One analysis was performed using *post mortem* human brain tissue taken from the intersection parietal to occipital cortex area from 8 control subjects and 8 patients with liver cirrhosis and accompanying HE. Tissue was provided by the body donor program of the Department of Anatomy at the Heinrich Heine University Düsseldorf, Germany. Additional *post mortem* human brain tissues from three patients with liver cirrhosis without HE were obtained from the Australian Brain Donor Programs NSW Tissue Resource Centre. A second Agilent™ whole human genome microarray analysis was performed using *post mortem* brain samples taken from the fusiform gyrus from control subjects, patients with liver cirrhosis with or without HE; each four cases [30]. Tissue was provided by the Australian Brain Donor Programs NSW Tissue Resource Centre. Gene array data was deposited at the public genomic data repository GEO (GSE41919 and GSE57193).

## 2.13. Statistical analysis

Data are presented as mean  $\pm$  standard error of the mean (SEM) unless stated otherwise. To test for statistical differences between two conditions an unpaired student's *t*-test was used. For other analyses, one-way ANOVA with Bonferroni's, Tukey's or Sidak's *post-hoc* test was applied as indicated in the figure legends.

## 2.14. Ethics statement

All Animals were treated and all experiments on them were performed in compliance with our institution's guiding principles "in the care and use of animals" in accordance with German animal protection law, and the EU Directive 2010/63/EU. Treatment protocols were reviewed and approved by the appropriate authorities (LANUV, Recklinghausen, Germany).

## 3. Results

### 3.1. Autophagic flux is modulated by ammonia in primary rat astrocytes

To test whether hyperammonemia affects autophagy, we used an established *in vitro* model of HE, namely treatment of primary rat astrocytes with  $\text{NH}_4\text{Cl}$  concentrations up to 5 mM [26],[31]. This concentration used in further settings shows no or only very minor toxicity as demonstrated by two assays (MTT- and Trypan blue-assay) (Fig. S1) and is similar to 5.4 mM found in brain tissue of rats subjected to portocaval anastomosis and hepatic artery ligation, an established *in vivo* rat model of HE [32]. First, primary rat astrocytes were transfected with pEGFP-LC3 and treated with increasing amounts of  $\text{NH}_4\text{Cl}$  for 72 h with or without chloroquine (CQ). CQ blocks autophagy and allows to test to which extent markers such as p62 or LC3 accumulate under a given situation. This is a commonly used measure of ongoing autophagic flux. In the absence of CQ we observed a dose-dependent increase in the accumulation of free GFP cleaved from GFP-LC3 demonstrating induction of autophagy by  $\text{NH}_4\text{Cl}$  (Fig. 1a). Moreover, endogenous LC3-II, the lipidated form of LC3 which is a well-established alternative marker for autophagy, accumulated upon addition of ammonia. At moderate concentrations (0.5 and 1 mM) of  $\text{NH}_4\text{Cl}$  (in the absence of CQ), we observed a pronounced accumulation of LC3-II indicating that autophagy is stimulated at these concentrations of ammonia

(Fig. 1a-c). Chloroquine treatment led to a pronounced accumulation of LC3-II when compared to the respective condition without CQ clearly demonstrating that autophagic flux occurs at these moderate ammonia concentrations. The accumulation of LC3-II is maximal at a concentration of 5 mM  $\text{NH}_4\text{Cl}$  and is nearly as strong in the absence of CQ as in its presence. The latter demonstrates that autophagy is efficiently blocked at 5 mM  $\text{NH}_4\text{Cl}$  independent of the presence of CQ.

Consistent with these findings, the accumulation of p62 (SQSTM1), an autophagy adaptor protein known to be degraded efficiently during autophagy, was observed with 5 mM  $\text{NH}_4\text{Cl}$  treatment (without CQ) further confirming the efficient inhibition of autophagic flux upon addition of ammonia. Treatment with 0.5 or 1 mM  $\text{NH}_4\text{Cl}$  as well as with rapamycin, an mTOR1 kinase inhibitor and known inducer of autophagy, led to a reduction in p62 levels. This confirms again that at moderately increased concentrations of ammonia (0.5 and 1 mM) autophagic flux is actually induced (Fig. 1a-c). Thus, moderately increased concentrations of  $\text{NH}_4\text{Cl}$  induce autophagy while a high concentration (5 mM) of  $\text{NH}_4\text{Cl}$  inhibits autophagic flux in primary rat astrocytes. These observations were corroborated using a fluorescence microscopy-based assay showing a statistically significant accumulation of GFP-LC3-positive structures at 5 mM  $\text{NH}_4\text{Cl}$  (Fig. 1d, e).

A more detailed characterization of the ammonia-induced autophagy inhibition in astrocytes revealed that the threshold concentration for  $\text{NH}_4\text{Cl}$  causing an inhibitory effect on autophagy after 72 h was in the range between 2 to 3 mM as already at these concentrations LC3-II accumulates strongly (Fig. 2a). When using 5 mM  $\text{NH}_4\text{Cl}$ , inhibition of autophagic flux is weakly detectable after 24 h and becomes very prominent after 48 and 72 h (Fig. 2b). The co-treatment with CQ shows an additive effect at all concentrations up to 4 mM  $\text{NH}_4\text{Cl}$  and at time points 24 h and 48 h suggesting that ammonia efficiently inhibits autophagy but does not block it completely under these conditions (Fig. 2a, b). Examination after early time points revealed that 5 mM  $\text{NH}_4\text{Cl}$  leads to an accumulation of p62 and LC3-II starting already after only one hour of treatment (Fig. 2c) demonstrating that hyperammonemia inhibits autophagic flux in primary rat astrocytes rapidly. This is reversible as we see a clear loss of p62 and LC3-II accumulation after a short washout period, starting after only 2 h and reaching control levels at approximately 12 h for both markers (Fig. 2d). We also confirmed that high ammonia concentrations are able to inhibit autophagy efficiently in various tumor cell lines both nervous tissue-derived and non-nervous tissue-derived (Fig. 2e) consistent with earlier studies [22],[33].

### 3.2. Inhibition of autophagy and impairment of lysosomal function is mediated by alteration of intralysosomal pH at high ammonia concentrations

Next, we tested whether administration of  $\text{NH}_4\text{Cl}$  impairs the formation of acidic lysosomes by increasing the pH explaining the observed block in autophagy. Applying LysoSensor™ Green DND-189 (Invitrogen) revealed a significant reduction (by ~50%) of the number of acidic lysosomes within cultured rat astrocytes after prolonged treatment with 5 mM  $\text{NH}_4\text{Cl}$  (Fig. 3a, b). This strongly supports the idea that elevated pH within lysosomes is the underlying mechanism for autophagy inhibition under hyperammonemia. To further evaluate the effect of ammonia on the number of autophagosomes/autolysosomes in primary rat astrocytes standard transmission electron microscopy (EM) was employed. We observed that 5 mM  $\text{NH}_4\text{Cl}$  treatment led to an increase of roughly 5-fold in the number of autophagosomes/autolysosomes compared to the water-treated control (Fig. 3c, d). A very similar increase was observed when applying 5 mM of the pH-mimetic compound  $\text{CH}_3\text{NH}_3\text{Cl}$ . This compound cannot be metabolized but alters cellu-

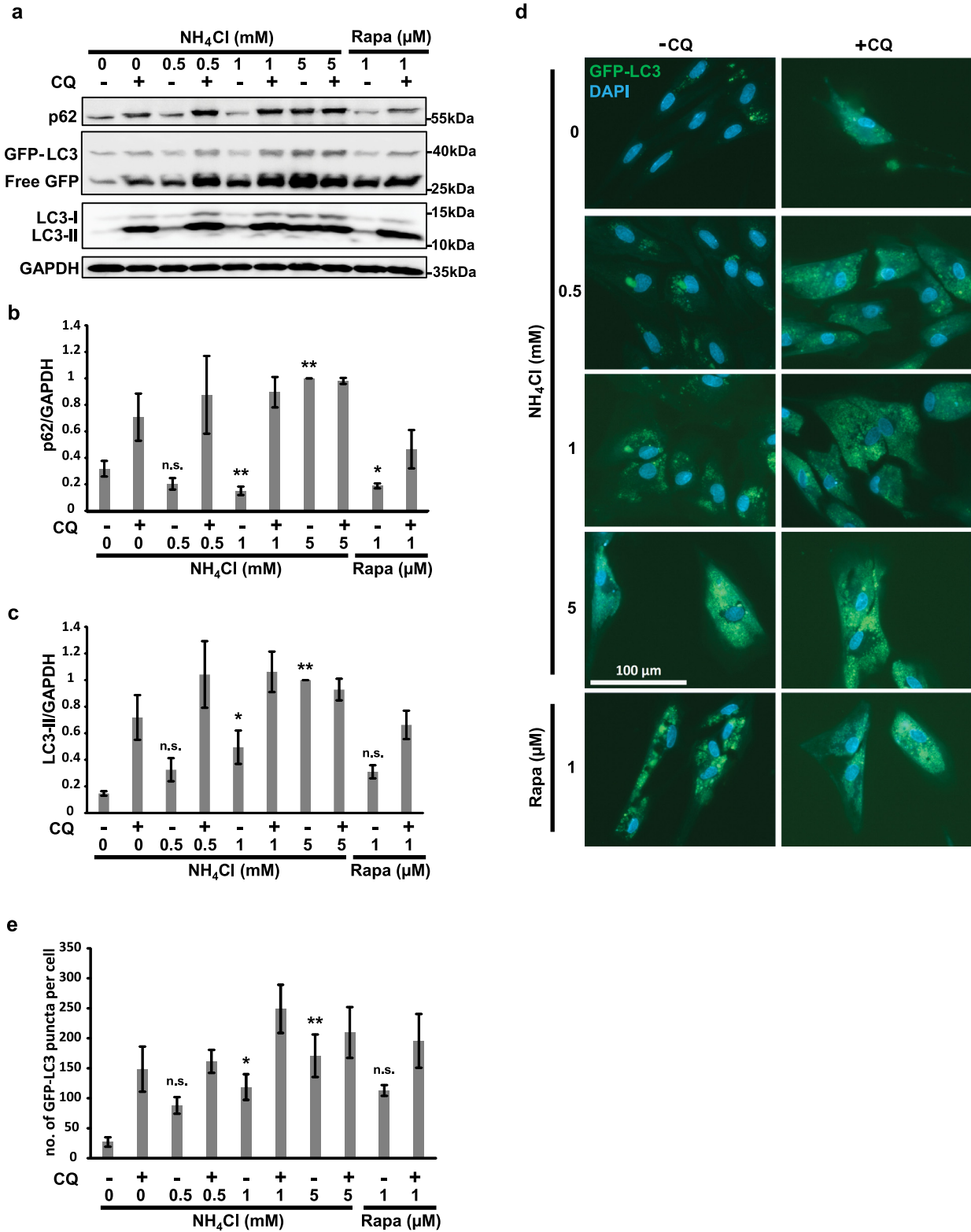


**Fig. 1. Autophagic flux is modulated by ammonia in cultured primary rat astrocytes.** Astrocytes were transfected with pEGFP-LC3 for 24 h, subsequently treated with indicated concentration of NH<sub>4</sub>Cl with or without chloroquine (CQ, 10 μM) for 72 h. Controls were left untreated for 48 h or autophagy was induced with rapamycin (Rapa, 1 μM) for 24 h. Autophagic activity was assayed by (a) WB and quantitative densitometry of endogenous autophagy markers (b) p62 and (c) LC3 (*n* = 3). (d) Representative fluorescence microscopy images of autophagosome formation indicated by GFP-LC3 puncta and of nuclei by DAPI staining (scale bar 100 μm). (e) Quantification of GFP-LC3 puncta per cell from 4 – 18 cells per condition. All graphs show mean ± SEM. Statistical analysis done with One-Way-ANOVA, followed by Bonferroni *post-hoc* test. \* *p* < 0.05, \*\* *p* < 0.01, n.s. not significant compared to ctrl (0 mM NH<sub>4</sub>Cl).

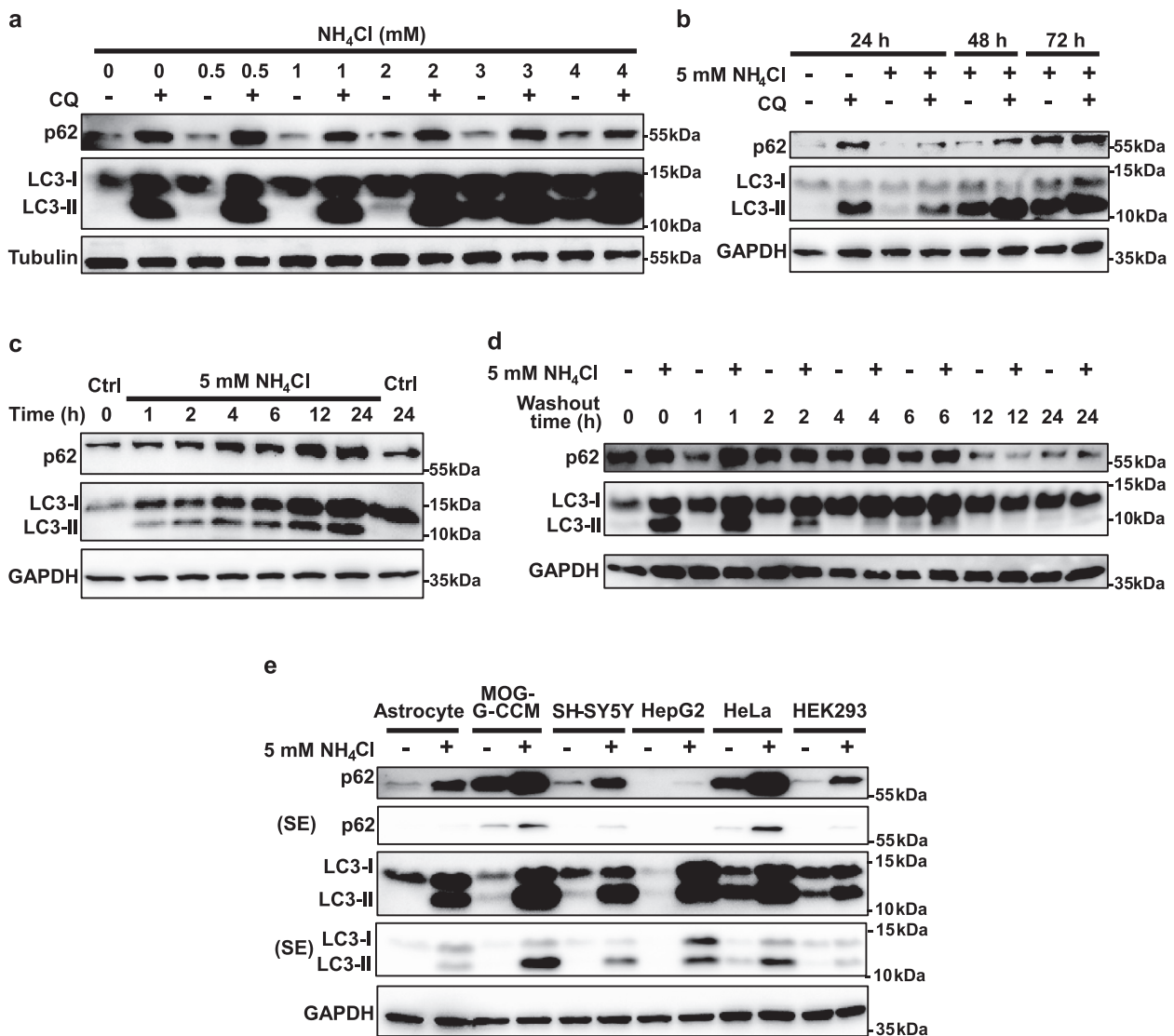


**Fig. 2. Autophagy inhibition by ammonia is time- and concentration-dependent, and reversible.** WB analysis of autophagy markers in astrocytes treated with various concentrations of NH<sub>4</sub>Cl with or without chloroquine (CQ, 10 μM) for indicated times to test (a) threshold concentration of autophagy inhibition, (b) time dependence, and (c) starting time point for autophagy inhibition. (d) Reversibility of autophagy inhibition induced by ammonia was assayed via WB after treatment of astrocytes with 5 mM NH<sub>4</sub>Cl for 72 h, followed by replacement of the medium with fresh medium lacking NH<sub>4</sub>Cl for indicated times. (e) WB analysis of autophagy markers in primary rat astrocytes and various human cell lines after 5 mM NH<sub>4</sub>Cl treatment for 72 h. SE, short exposure.

lar pH in a very similar manner as NH<sub>4</sub>Cl. Our results demonstrate that inhibition of autophagy is largely mediated by changes in intracellular and intralysosomal pH. Neither CH<sub>3</sub>NH<sub>3</sub>Cl nor NH<sub>4</sub>Cl, however, did alter the average size or perimeters of autophagosomes/autolysosomes significantly (Fig. 3e, f and S2b–g), yet led in few cases to quite large autophagosomes consistent with an accumulation of engulfed material (Fig. S2a). To test whether altering intralysosomal pH (Fig. 3a and b) indeed impairs lysosomal activity during autophagy we determined cathepsin L activity in cultured rat astrocytes treated with CH<sub>3</sub>NH<sub>3</sub>Cl or NH<sub>4</sub>Cl for 48 h. Activity of lysosomal degradation enzymes including cathepsin L is strongly dependent on the acidic environment of the lysosome [34]. Both, CH<sub>3</sub>NH<sub>3</sub>Cl and NH<sub>4</sub>Cl triggered a roughly 2-fold reduction of cathepsin L activity (Fig. 3g) in line with the conclusion that lysosomal activity is severely impaired due to an increase of intralysosomal pH. WB analysis further confirmed that CH<sub>3</sub>NH<sub>3</sub>Cl is sufficient to inhibit autophagy to a similar extent as NH<sub>4</sub>Cl since both p62 and LC3-II accumulate to a similar extent upon administration of the two compounds (Fig. 4a–c).

### 3.3. Ammonia-induced inhibition of autophagy occurs in a ROS-dependent manner

Previous studies suggested a significant contribution of ROS in the pathogenesis of HE using different *in vitro* and *in vivo* models [6–8] prompting us to investigate the role of ROS in respect to our findings on impaired autophagy. Upon administration of NAC, an intracellular ROS scavenger, ammonia-induced accumulation of p62 and LC3-II was largely abolished (Fig. 4a–c) suggesting that inhibition of autophagic flux depends on the formation of ROS. Likewise, the addition of apocynin, an inhibitor of NADPH oxidases, prevented accumulation of p62 and LC3-II in NH<sub>4</sub>Cl-treated astrocytes (Fig. S3) supporting this conclusion. However, co-treatment of astrocytes with NH<sub>4</sub>Cl and the glutamine synthetase (GS) inhibitor MSO, or the p38MAPK inhibitor SB203580, showed little or no alleviation on autophagy inhibition suggesting that ammonia-induced autophagy inhibition is independent of GS or p38MAPK (Fig. 4a–c, and Fig. S3). These findings were confirmed using immunostaining of LC3 and fluorescence microscopy

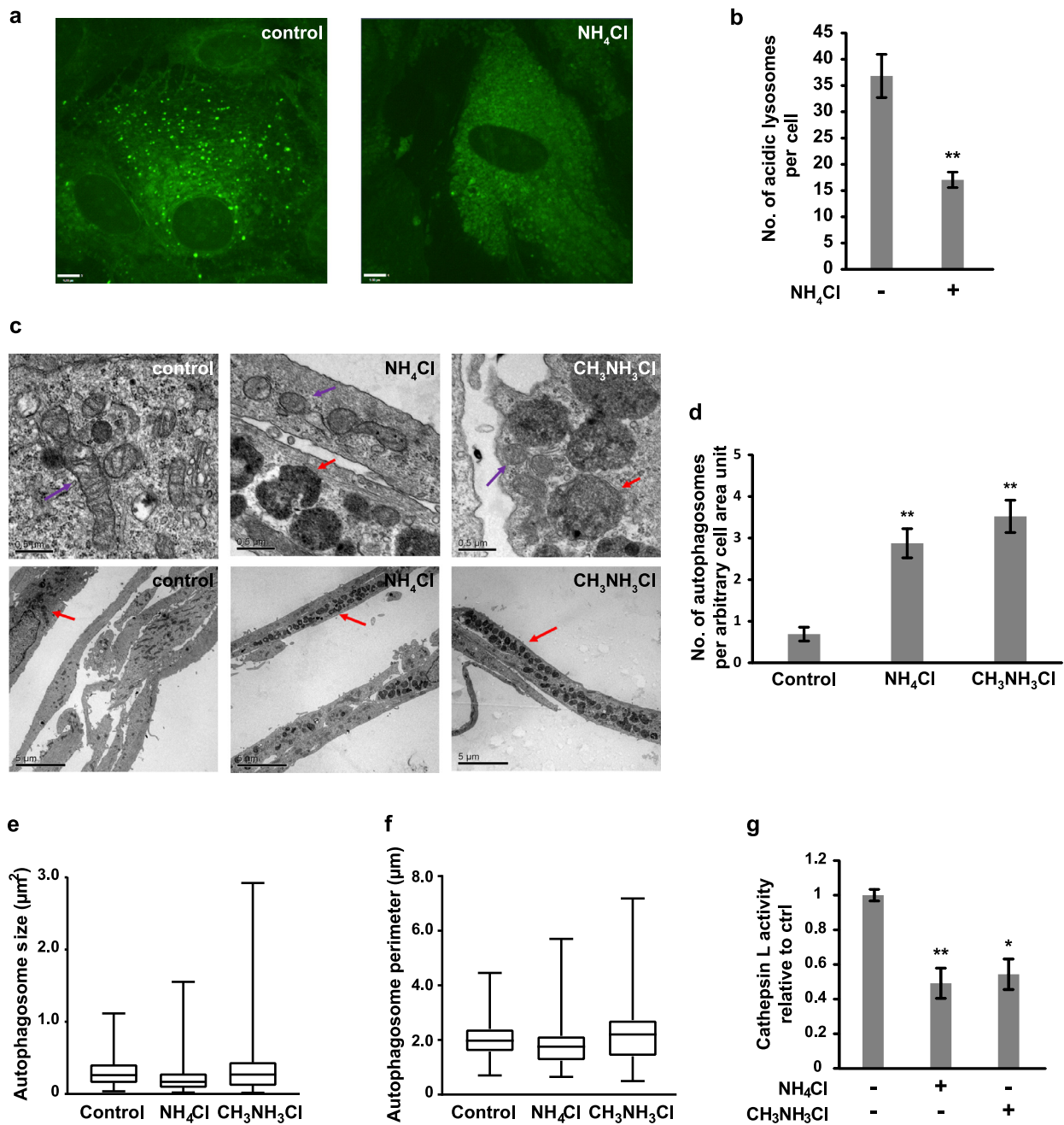


**Fig. 3. Ammonia impairs lysosomal function and induces accumulation of autophagosomes.** (a) Representative fluorescence microscopy pictures of LysoSensor<sup>TM</sup>-treated astrocytes (scale bar: 9 µm) and (b) quantification of acidic lysosomes per cell (>50 cells per condition). (c) Representative EM pictures of autophagosomes in cultured primary rat astrocytes treated with indicated substances for 72 h (red arrows, autophagosomes/lysosomes; purple arrows, mitochondria; scale bars: 0.5 µm upper images, 5 µm lower images). (d) Quantification of autophagosome number per arbitrary cell area unit, (e) autophagosome size, and (f) perimeter, ( $n = \approx 40$  images for each group). (g) Magic Red<sup>TM</sup> cathepsin L activity assay of astrocytes treated with indicated substance for 72 h ( $n = 3$ , normalized to ctrl). Graphs b, d, and g show mean  $\pm$  SEM, graphs e and f show quartiles. Statistical analysis done using two-tailed student's *t*-test for panel b and One-Way-ANOVA, followed by Bonferroni *post-hoc* test for d and g. \*  $p < 0.05$ , \*\*  $p < 0.01$ .

which showed reduced accumulation of LC3 puncta upon addition of NH<sub>4</sub>Cl when using NAC but not MSO or SB203580 (Fig. 4d, e). Addition of CH<sub>3</sub>NH<sub>3</sub>Cl was sufficient to cause accumulation of LC3 puncta. Also, similar to NH<sub>4</sub>Cl, the inhibitory effect of CH<sub>3</sub>NH<sub>3</sub>Cl on autophagy was fast, reversible, and could be prevented by intracellular ROS scavengers, once more indicating that the mode of action of both NH<sub>4</sub>Cl and CH<sub>3</sub>NH<sub>3</sub>Cl is the same (Fig. S4a–c). These results show that ammonia-induced inhibition of autophagy is a pH-mediated but not a GS-, or p38MAPK-dependent process. Overall, we conclude that ammonia-induced effects on autophagy are mediated by altering the intracellular/lysosomal

pH and depend, at least partially, on intracellular formation of ROS.

#### 3.4. Autophagy is modulated in the brain of HE patients and in animal HE models

Transglutaminase 2 (TGM2) is strongly upregulated under various stress conditions including tissue injury, inflammation, protein misfolding, and oxidative stress and was shown to positively regulate late steps of autophagy [35],[36]. We checked whether protein levels of TGM2 were increased in cultured rat astrocytes

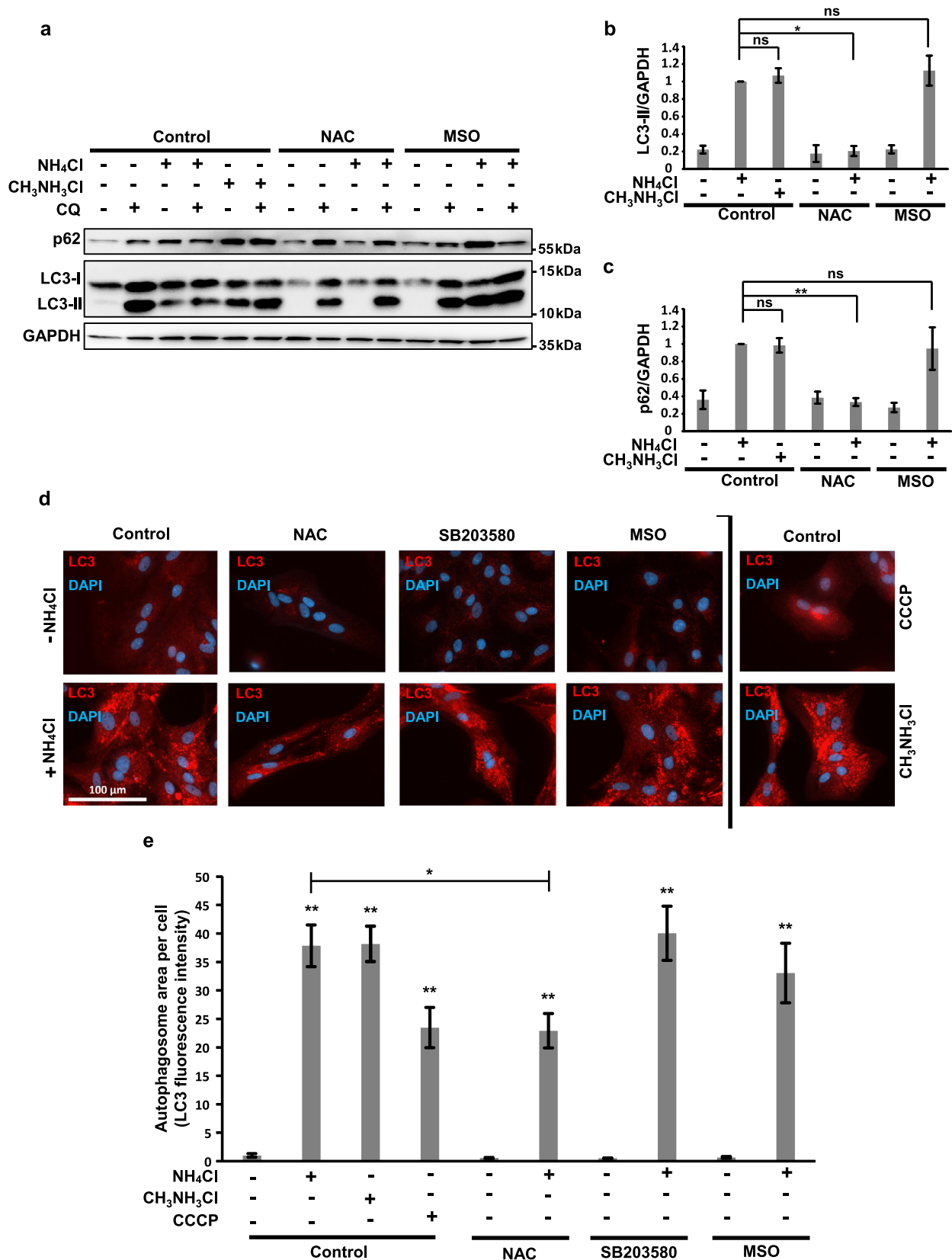


**Fig. 4. Ammonia-induced inhibition on autophagy is mediated by changes in intracellular pH and depends on ROS.** When indicated astrocytes were pre-treated with the glutamine synthetase (GS) inhibitor MSO (3 mM), or the ROS scavenger NAC (2 mM), or the p38MAPK inhibitor SB203580 (10  $\mu$ M) for 30 min followed by a treatment with NH<sub>4</sub>Cl (5 mM), CH<sub>3</sub>NH<sub>3</sub>Cl (5 mM), or H<sub>2</sub>O (control) with or without chloroquine (CQ, 10  $\mu$ M) for 72 h. Chemicals used for pretreatments remained present during subsequent steps. CCCP (10  $\mu$ M) for 30 min was used as a control. (a) WB and densitometry of autophagic markers (b) LC3 and (c) p62 ( $n = 3-4$ ). (d) Representative IF microscopy images for detection of endogenous LC3 (red; LC3; blue: DAPI; scale bar: 100  $\mu$ m), (e) quantification of autophagosomal area per cell from panel d. Graphs show mean  $\pm$  SEM. Statistical analysis done with One-Way-ANOVA, followed by Bonferroni *post-hoc* test. \*  $p < 0.05$ , \*\*  $p < 0.01$ , ns: not significant.

upon treatment with  $\text{NH}_4\text{Cl}$  and whether TGM2 could be used as an additional marker of altered autophagy. Indeed, TGM2 was increased in a concentration- and time-dependent manner in primary rat astrocytes (Fig. S5a, b) and an increase was also evident in HepG2 cells (Fig. S5c). To test whether autophagy is modulated *in vivo* we next checked whether mRNA levels of TGM2 are altered in humans suffering from HE. Data from two patient cohorts subjected to whole genome microarray analyses confirmed that TGM2 gene expression was increased significantly ~3-fold in *post mortem* human brains from liver cirrhosis patients with HE compared to controls (patients without cirrhosis) or compared to liver cirrhosis patients without HE (Fig. 5a, top and bottom panels). This is consistent with an animal *in vivo* HE model as TGM2 protein levels were also increased in the cerebral cortex of rats exposed to  $\text{NH}_4\text{Ac}$  compared to control brain samples (Fig. 5b, c). Moreover, we see a significant increase in the protein level of the autophagy marker LC3 in *post mortem* human brains from liver cirrhosis patients with HE compared to controls (patients without cirrhosis) as well as compared to liver cirrhosis patients without HE (Fig. 5d, e). Overall, we provide several lines of evidence that hyperammonemia in the brain results in modulation of autophagic flux *in vivo* pointing to a role of autophagy in the pathogenesis of HE.

### 3.5. Taurine alleviates the degree of autophagy impairment caused by hyperammonemia in primary rat astrocytes and in an animal model of HE

The beta-amino sulfonic acid taurine has been demonstrated to be potent in preventing ammonia-induced proliferation inhibition and senescence in astrocytes [13],[26] and to alleviate liver injury and brain edema in animal HE models [37],[38]. We thus asked whether taurine could act via modulating autophagy. Indeed, cultured primary rat astrocytes exposed to taurine treatment showed a reduced autophagy inhibition upon addition of ammonia compared to untreated astrocytes as accumulation of LC3-II and p62 were significantly reduced in the presence of taurine (Fig. 6a, b and Fig. S6a, compare lane 3 vs. 7). This observation of significantly reduced levels of p62 could indicate that taurine promotes autophagic flux despite the presence of high ammonium concentrations. Thus, we quantified the autophagic flux using an established method based on the relative accumulation of p62 or LC3-II caused by addition of CQ. Consistent with our data shown above (Fig. 1a-c and Fig. 2a-c) 5 mM  $\text{NH}_4\text{Cl}$  is sufficient to block autophagy nearly completely as CQ only results in a marginal additional accumulation of p62 or LC3-II (Fig. 6a, b and Fig. S6a, compare lane 3 vs. 4). However, in the presence of taurine adding CQ results in a clear further accumulation of p62 or LC3-II despite the presence of 5 mM  $\text{NH}_4\text{Cl}$  (Fig. 6a, b and Fig. S6a, compare lane 7 vs. 8). Thus, autophagic flux is significantly increased by taurine under conditions of hyperammonemia (Fig. 6c and Fig. S6b).

To test whether inhibition of autophagy also occurs *in vivo* and whether taurine shows similar effects we used an established rat model of acute hyperammonemia in which an increase of ammonia levels in the blood was induced by intraperitoneal administration of  $\text{NH}_4\text{Ac}$  to Wistar rats. Alterations of autophagy *in vivo* were evaluated by analyzing tissue protein lysates obtained from the cerebral cortex of rats with or without acute ammonium intoxication (Fig. 6d, e). 24 h after  $\text{NH}_4\text{Ac}$  administration, prominent conversion of LC3-I to LC3-II as well as accumulation of LC3-II and p62 were observed demonstrating that autophagy impairment induced by ammonia occurs in rat brain. Rats receiving taurine supplement showed a rather moderate autophagy inhibition in the cortex as evidenced by a minor non-significant accumulation of p62 (Fig. 6f, g right panel). LC3-II showed a significant but limited accumulation (Fig. 6f, g left panel). The inhibition of autophagy

by hyperammonemia in rats receiving taurine was thus apparently less compared to rats not receiving taurine (Fig. 6d, e vs. 6f, g). To validate this in a quantitative manner and due to the fact that *in vivo* we cannot determine autophagic flux by CQ administration, we determined the relative inhibition of autophagy by ammonia in the presence vs. in the absence of taurine. Indeed, we observed that taurine is able to alleviate ammonia-induced inhibition of autophagy significantly also in the *in vivo* HE model (Fig. 6h) consistent with the *in vitro* HE model shown above (Fig. 6a-c). These results confirmed the *in vivo* relevance of the ammonia-induced autophagy inhibition and the protective effect of taurine via modulation of autophagy. The latter provides a novel rationale for the mode of action of taurine.

### 3.6. Neurons show impairment of autophagy under hyperammonemia

To investigate the effects of ammonia also on neurons we used an established mouse primary neuron-glia cell co-culture model [24],[25]. After 72 h of 5 mM ammonia intoxication a significant increase in LC3-II accumulation was detected in total cell extracts derived from neurons co-cultured with astrocytes (Fig. 7a, b). When we tested the effect of taurine in this context, we still observed an ammonia-induced accumulation of LC3-II, yet the extent of this accumulation was moderately reduced compared to the condition without taurine (Fig. 7a, b). To exclude that the LC3 signal in these cell extracts is partly derived from glia cells, we also performed immunofluorescence staining and analyzed the accumulation of LC3 clusters specifically in MAP2-positive neurons (Fig. 7c, d). Consistent with our earlier data, we observed a clear ammonia-induced increase of the number of LC3 clusters suggesting a block in autophagy in MAP2-positive neurons. This accumulation again appeared to be moderately reduced by taurine ( $p=0.07$ ) suggesting that taurine can alleviate ammonia-induced impairment of autophagy also in neurons. The result that taurine alone caused an apparent accumulation of LC3 (Fig. 7c, d) can be attributed to a gross accumulation of LC3 clusters in the nucleus of various, yet not all, cells. The functional significance of nuclear LC3 clusters is unclear and future studies have to address this and the effect of taurine on neuronal autophagy in general.

Expanding these observations to our *in vivo* model system, brain sections from different brain areas of acutely  $\text{NH}_4\text{Ac}$ -intoxicated Wistar rats were prepared and immunostained for LC3 and cell type-specific markers. In the corpus callosum, an area mainly inhabited by glia cells, a noticeable increase in total LC3 fluorescence was observed (Fig. 7e, g), confirming the results from the WB analysis of rat brain lysates. In the cerebral cortex however, an area of roughly equal amounts of neurons and glia cells, we did not observe a significant increase in total LC3 fluorescence, despite the fact that apparently a few cells appeared to show increased LC3 levels (Fig. 7f, h). Overall, we provide experimental evidence indicating that next to astrocytes autophagy is also impaired by hyperammonemia in neurons, possibly to varying degree in certain regions in the brain.

### 3.7. Taurine does not appear to modulate mTOR-dependent autophagy signaling but alleviates ammonia-induced ROS formation

Our data strongly point to a role of taurine in modulating autophagic flux. Thus, we aimed to investigate the underlying basic molecular mechanism using an astrocytoma cell culture. One well-known and important pathway to induce autophagy is via inactivation of the mTORC1 complex which can be monitored by dephosphorylation of mTORC1. Taurine treatment alone or together with ammonia for 72 h did not result in dephosphorylation of mTORC1 suggesting that taurine does not cause inhibition of mTORC1. As a

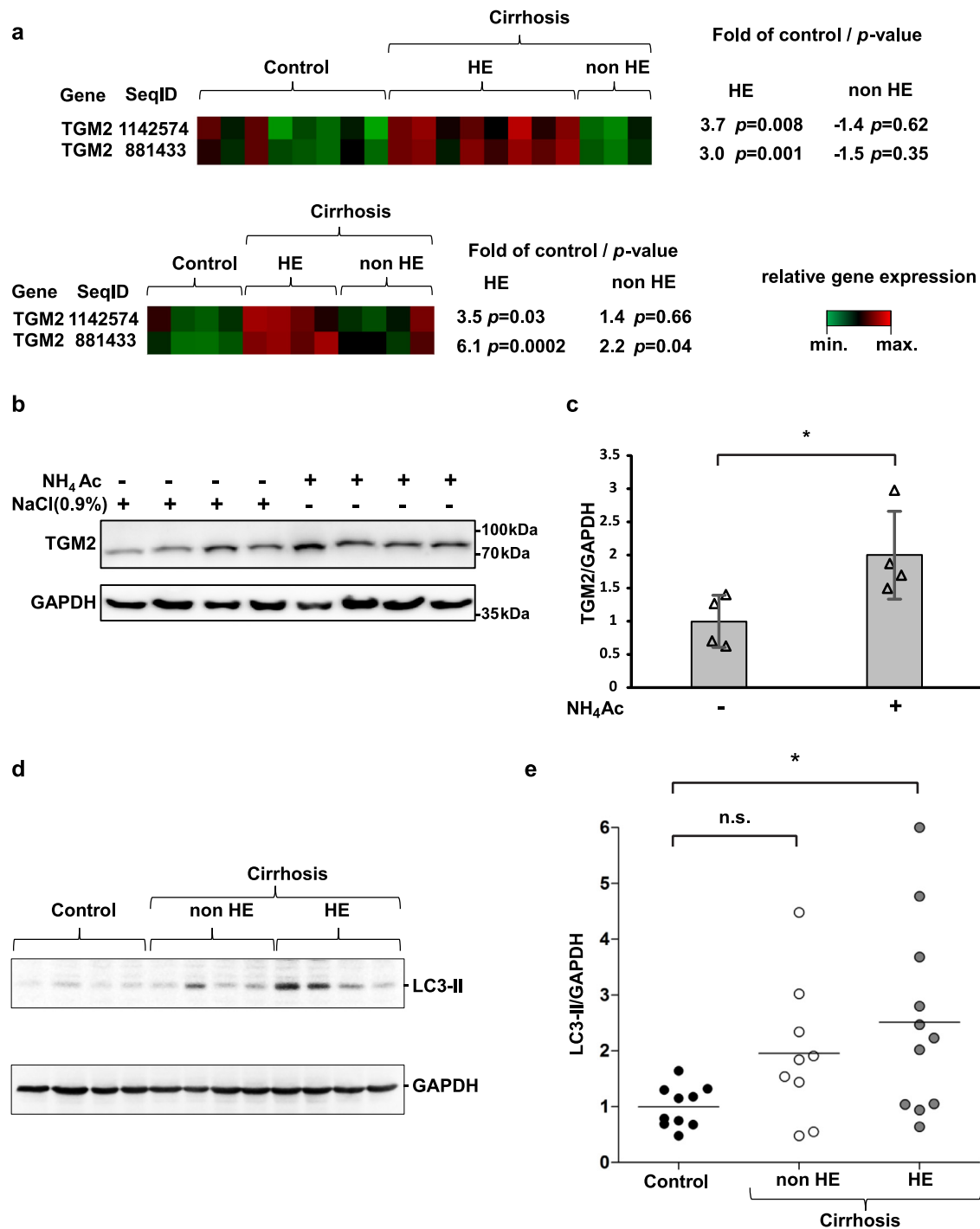


**Fig. 5. Autophagy is modulated in HE Patients and in animal HE models.** (a) TGM2 gene expression levels determined by microarray analysis in the cerebral cortex of patients with liver cirrhosis with or without HE and controls (two independent patient cohorts, top and bottom panels). Fold-changes and *p* values compared with control groups are indicated. Red, enhanced; green, reduced gene expression. (b) WB of TGM2 in cerebral cortex samples from rats after acute ammonium intoxication (NH<sub>4</sub>Ac administration, 4.5 mmol/kg BW, 24 h). (c) Densitometry of panel b. Average fold change as well as individual values of TGM2/GAPDH are presented. \* *p* < 0.05. (d) Representative WB of LC3-II using protein lysates prepared from human *post mortem* brain biopsies from controls and patients with liver cirrhosis with or without HE and control. (e) Densitometric quantification of LC3 II levels normalized to the mean of ctrls. Graph shows single values and mean, graph c also shows mean ± SD. Statistical analysis done with One-Way-ANOVA, followed by Dunnett's *post-hoc* test. \* *p* < 0.05, \*\* *p* < 0.01, n.s. not significant.

control we used Torin2, a well-known inducer of autophagy causing inactivation and concomitant dephosphorylation of mTORC1 (Fig. S8a). Autophagy can also be induced via the MAPK(Erk1/2) pathway in a mTORC1-dependent and -independent manner. Here we observed that MAPK (Erk1/2) shows no alteration of its phosphorylation state after taurine treatment (Fig. S8a) suggesting that taurine does not modulate autophagy via this pathway either. As a

control we confirmed that Torin 2 also promoted phosphorylation of MAPK (Erk1/2) to induce autophagy. Dephosphorylation of Atg13 is another marker of autophagy induction via mTORC1-inhibition. Probing for phosphorylation changes of Atg13 revealed no gross changes by ammonia with or without taurine corroborating the view that mTOR1 signaling is not modulated here. In a complementary approach using primary rat astrocytes and immunoflu-

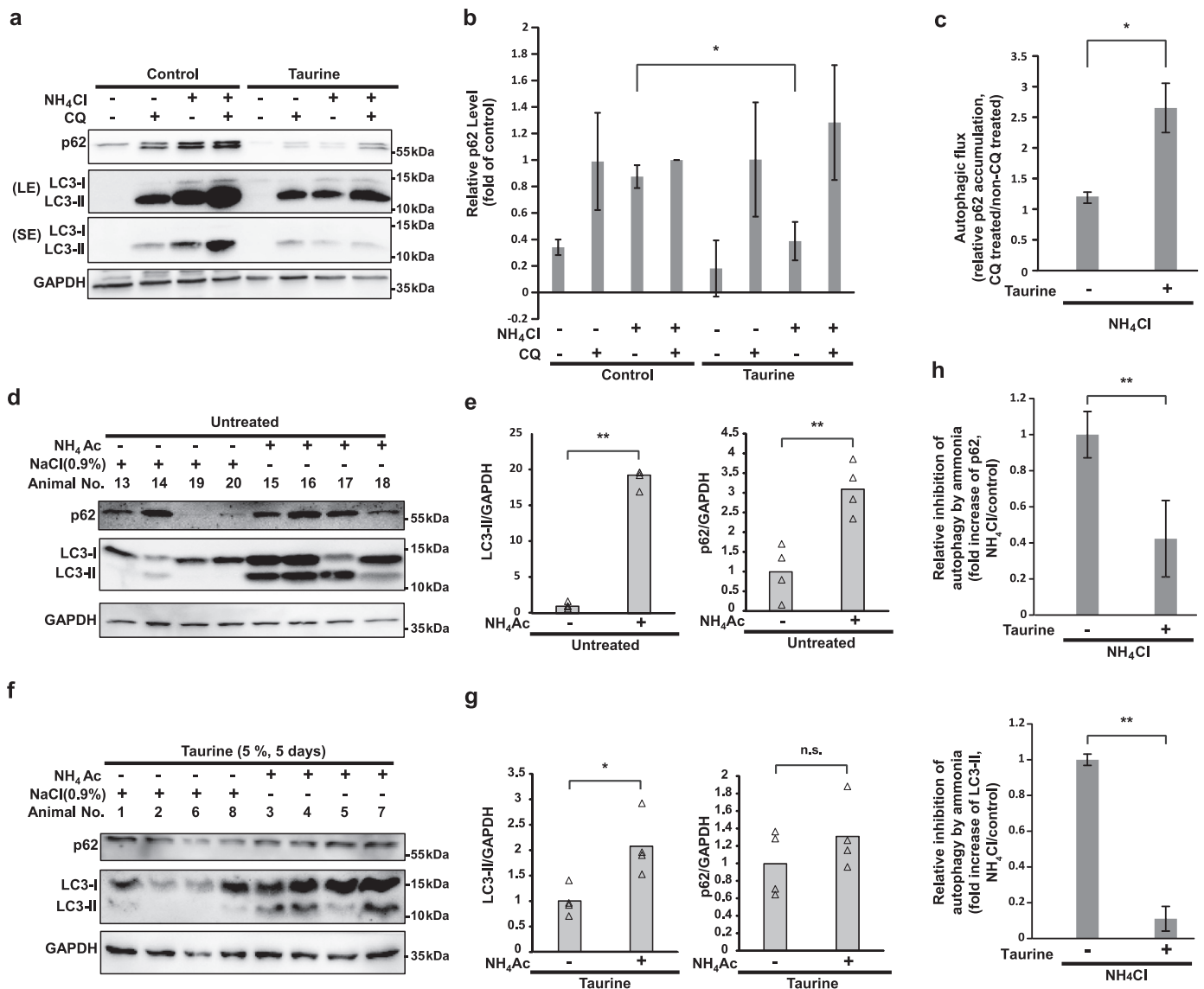


**Fig. 6. Taurine alleviates the degree of autophagy impairment caused by hyperammonemia *in vitro* and *in vivo*.** (a) Representative WB of autophagy markers in astrocytes pre-treated 30 min with 5 mM taurine when indicated and treated with NH<sub>4</sub>Cl (5 mM) and/or CQ when indicated. LE/SE; long/short exposure. (b) Densitometry of p62 levels ( $n = 3-6$ , each normalized to NH<sub>4</sub>Cl+CQ control). (c) Quantification of autophagic flux as represented by relative fold change of p62 accumulation caused by CQ treatment. (d) WB analysis of cerebral cortex samples from a rat model of acute ammonium intoxication (NH<sub>4</sub>Ac administration, 4.5 mmol/kg BW, 24 h); (e) Densitometry of panel d. LC3-II/GAPDH (left) or p62/GAPDH (right) are presented relative to ctrl. (f) WB analysis of the same model with pretreatment of taurine supplement (5% taurine in drinking water for 5 days). (g) Densitometry of panel f. LC3-II/GAPDH (left) or p62/GAPDH (right) are presented relative to ctrl. (h) Relative inhibition of autophagy by ammonia as represented by relative fold change of p62 (top) or LC3-II (bottom) accumulation caused by NH<sub>4</sub>Ac administration *in vivo* in the absence vs. presence of taurine. Graphs b, c, and h show mean  $\pm$  SEM, graphs e, and g show individual values and mean. Statistical analysis done with two-tailed student's *t*-test. \*  $p < 0.05$ , \*\*  $p < 0.01$ , n.s. not significant.

orecence we checked whether taurine induces the formation of Atg16L or WIPI2 puncta, both indicators for early stages of autophagy. Neither Atg16L, nor WIPI2 showed a drastically different staining pattern i.e. puncta formation or colocalization, whereas the control using Torin 2 -treated did (Fig. S8c), indicating that taurine does not grossly affect these early steps in autophagy induction. Next, we asked whether the reported antioxidative property of taurine may impair autophagy induction. We determined ROS using CellROX™ green in astrocytoma cells after 72 h without treatment (control), or with ammonia, taurine, or in combination (Fig. S8d, e). Consistent with earlier reports ammonia caused a significant increase of cellular ROS compared to control cells. The increase in ROS caused by ammonia was almost completely prevented by co-treatment with taurine showing ROS level comparable to ctrl cells and to cells treated with taurine alone (Fig. S8d, e). This strongly suggests that the known ROS scavenging effect of

taurine contributes to the observed modulation of autophagy in astrocytes.

#### 4. Discussion

In the present study we analyzed the effects of hyperammonemia on autophagy in the brain using well established *in vitro* and animal HE models and also in humans suffering from HE. We show for the first time that autophagy is strongly inhibited in these HE models using different independent experimental approaches such as WB analysis, fluorescence microscopy, and electron microscopy. This occurs in a time- and concentration-dependent manner and is fully reversible in cultured astrocytes. The mechanism by which ammonia modifies the progression of autophagy is shown to be dependent on the alteration of the intracellular pH as well as on the generation of ROS. These findings are expanded *in vivo* us-

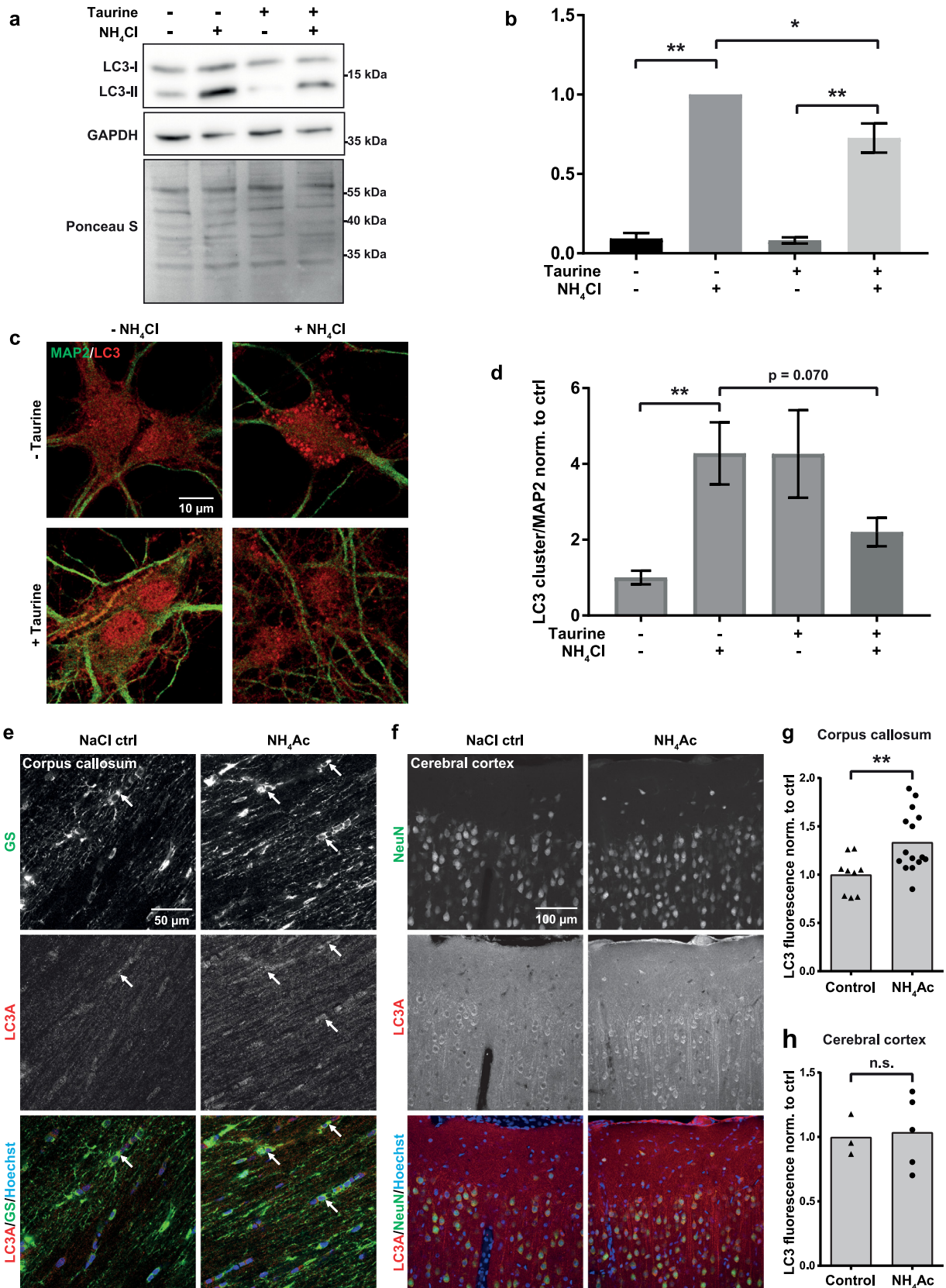


**Fig. 7. Neurons show a moderate autophagy impairment by hyperammonemia.** (a-d) Neurons in upside-down co-culture with glia cells were treated with 5 mM NH<sub>4</sub>Cl for 72 h and/or 5 mM Taurine (30 min prior to NH<sub>4</sub>Cl) and subjected to WB or IF analysis. (a) Representative WB of autophagy marker LC3. (b) Densitometry of 4 independent experiments each with 2–3 technical replicates normalized to loading control and to cells treated with 5 mM NH<sub>4</sub>Cl for 72 h alone. (c) Representative IF images (MAP2 stained with AlexaFluor488, LC3 with AberiorStar635P). (d) Quantification of LC3 cluster area divided by total MAP2 area normalized to ctrl. 29 – 38 cells from 3 to 4 independent experiments were analyzed. (e-h) Wistar rats were acutely intoxicated with 4.5 mmol/kg body weight of NH<sub>4</sub>Ac or NaCl ctrl for 24 h, sacrificed and their brain sections were analyzed by immunohistochemistry (IHC). (e) Representative IHC images from the corpus callosum and (f) the cerebral cortex. GS or NeuN as cellular specific markers were stained with FITC, LC3 with Cy3, and nuclei with Hoechst. (g-h) Quantification of total LC3 fluorescence per image from (g) corpus callosum (3 images per animal,

ing *post mortem* brain tissue from liver cirrhosis patients with HE showing a significant induction of the autophagy markers LC3-II as well as TGM2 which apparently does not occur in liver cirrhosis patients without HE or patients without liver cirrhosis. This is fully in line with the *in vitro* HE model using primary rat astrocytes as well as an *in vivo* animal HE model. One major advantage of the *in vitro* HE model clearly is the possibility to dissect the molecular mechanism of autophagy modulation in more detail and to study possible treatments reversing ammonia-induced toxicity. This allowed us for example to show that an increase in intracellular/lysosomal pH is a key factor in mediating the observed effects. Ammonia is known to increase the intracellular pH to levels which decrease lysosome protease activities [34],[39]. In line with this, we demonstrate that autophagy inhibition as well as loss of cathepsin L activity was mimicked by  $\text{CH}_3\text{NH}_3\text{Cl}$ , a non-metabolizable compound causing pH-changes similar as  $\text{NH}_4\text{Cl}$ . Furthermore, this fits well to our observation that ammonia-treated cultured rat astrocytes showed a reduced number of acidic lysosomes. At the same time, we observed an increase in the number of autophagosomal/lysosomal structures by EM which is expected under conditions when autophagic flux is inhibited as non-acidic lysosomes are impaired in their ability to efficiently degrade cellular waste material.

Many of the previously observed effects of ammonia on astrocytes have been attributed to the formation of ROS [1],[40]. Interestingly, this also applies to autophagy. Both the ROS scavenger NAC and the NADPH oxidase inhibitor apocynin were able to attenuate many of the observed effects pointing to a critical role of ROS for modulation of autophagy by ammonia. This is in line with earlier reports demonstrating that ROS are important signaling molecules required for the regulation of autophagy [41],[42]. Moreover, reducing ROS levels by ROS scavengers might simply reduce the amount of damaged cellular material that needs to be degraded via autophagy which consequently might lead to a lower accumulation of autophagosomes. Ammonia-induced ROS formation, as reported in earlier studies [8],[31], may also result in direct oxidation and inactivation of lysosomal enzymes which further impairs clearance by autophagy. All these ROS-mediated effects could explain the apparent reduction of ammonia-induced autophagy inhibition exerted by ROS scavengers.

The inhibition of autophagic flux under hyperammonemia could well explain the increase in the levels of LC3 and of the transglutaminase TGM2 *in vitro* and *in vivo* models as well as in *post mortem* brain samples of liver cirrhosis patients with HE. An upregulation at the mRNA level of TGM2 as observed here in HE patients indicates a response to counteract the effects of ammonia-induced stress as TGM2 is known to promote autophagy [35]. The increase in TGM2 was well recapitulated when analyzing *in vitro* and *in vivo* HE models. In accordance with the accumulation of autophagy markers p62 and LC3, TGM2 upregulation in cultured rat astrocytes was similarly time- and concentration-dependent, demonstrating a possible causal connection of autophagy inhibition and activation of the autophagy pathway possibly to overcome the inhibition. Interestingly, in neurons, TGM2 ablation was reported to result in increased vulnerability towards cellular stress [43]. It appears that TGM2 is a central player regulated by p53 that is induced by ammonia [31],[44], in order to trigger cellular stress responses. Still, future studies will have to elucidate to what extent TGM2 is mechanistically involved in the development of HE symptoms.

The general inhibitory effect of ammonia on autophagy is well known for a number of cell types including fibroblasts, liver cells

and tumor cell lines [21],[22], yet it has not been reported so far for astrocytes or brain tissue in HE and related models. Here we show that the inhibition of autophagy starts at concentrations as low as 2 mM and progresses with time and concentration. It should be noted that at moderately increased concentrations of ammonium (1 mM or lower) even a slight induction of autophagy occurs suggesting an initiation of a compensatory, pro-survival mechanism at these lower ammonia concentrations. This dual effect of ammonia is consistent with earlier results using tumor cell lines [33] and with the increase in TGM2 mRNA levels in human brain of HE patients. As a block in autophagy caused by hyperammonemia profoundly affects many HE relevant physiological and pathological processes such as cellular quality control and inflammation [45], it is expected that long-term, efficient autophagy inhibition in the brain, as reported here, will facilitate the pathogenesis and increase the severity of symptoms and lethality in HE. In line with this, decreased autophagosome biogenesis and inhibited autolysosome degradation were also observed in patient samples of various neurodegenerative diseases including Alzheimer's disease and Parkinson's disease [46]. Although astrocytes are the major and primary target of ammonia-induced toxicity during the pathogenesis of HE [1],[40] we also provide evidence that neurons are similarly impaired in their autophagic capabilities by hyperammonemia. Our *in vitro* glia-neuron co-culture model shows a clear ammonia-dependent increase of LC3-II in mouse neurons with two independent methods. For the Corpus callosum of ammonia-intoxicated rats a similar accumulation of LC3 under hyperammonemia was observed but not for the cortex suggesting brain region specific effects. This is not unexpected given the fact that the relative number of glia cells *versus* neurons is variable and that, moreover, the treatment times was short (24 h vs. 72 h in the *in vitro* approach). Furthermore, it is likely that the autophagy inhibition in neurons is cushioned by astrocytes *in vivo* much more effectively than in the co-culture model as in the latter case the ratio of astrocytes per neurons is lower. Overall, as ammonia is a highly diffusible and membrane-permeable molecule, it is quite likely that ammonia-induced harmful effects on autophagy also occur in neuronal cells *in vivo* (e.g. in a chronic hyperammonemia model) and at a pleiotropic tissue level, including the liver, which may result in negative systemic effects and thus contribute to the development of HE symptoms.

Current therapy options for HE are limited and largely target the production of ammonia in the intestine or the gut microbiome [1]. Combining our findings with earlier studies we now propose that alterations in autophagy in astrocytes are involved in the pathogenesis of HE as well, a view that has been neglected in the past. Restoring this process is therefore a possible, novel therapeutic strategy. A promising and well-known compound studied extensively in the past could be taurine. Here we demonstrate that taurine, a non-proteinogenic amino acid widely known as a biomembrane stabilizer and oxidative stress mitigator, largely abolishes ammonia-induced autophagy inhibition in different models of HE. These results shed new light on earlier studies showing that taurine is able to abolish ammonia-induced proliferation inhibition and senescence [13],[26], and to reduce liver injury and brain edema under conditions of hyperammonemia [37],[38]. Further, high serum taurine levels prior to treatment with L-carnitine were reported to be a positive predictor in patients suffering from minimal HE [47]. Here we provide several lines of evidence that taurine directly or indirectly promotes autophagic flux despite the presence of high concentrations of ammonia. This is demonstrated

3 – 5 animals) and (h) cerebral cortex (1 image per animal, 3 – 5 animals). Statistical analysis for panel b and d done using One-Way-ANOVA and Sidak's *post-hoc* test.  $\text{NH}_4\text{Cl}$ -Taurine to ctrl and  $\text{NH}_4\text{Cl}$ -Taurine to  $\text{NH}_4\text{Cl}$ +Taurine significance from panel b was determined by one-sample *t*-test. Statistical analysis for panel g and h done using two-tailed student's *t*-test. \*\*  $p < 0.01$ , \*  $p < 0.05$ , n.s. not significant.

*in vitro* as well as *in vivo* HE models and provides a novel rationale how taurine could act mechanistically. However, this effect of taurine does not appear to be the result of a direct, strong activation of autophagy via the well-known mTOR pathway. Possibly, the effect is much more subtle and thereby hard to detect or the flux increase is even mediated via a different signaling pathway. Our data point to an important role of taurine via alleviating ROS-dependent effects on autophagy. The exact molecular mechanism of taurine remains elusive. Taurine is known to be beneficial for many mitochondrial functions, e.g. it can stabilize mitochondrial matrix pH [48], it can assist in mitochondrial calcium homeostasis [49], and it was furthermore shown to reduce mitochondrial swelling and ROS generation in a rat HE model [50]. Since many studies have shown an impact of hyperammonemia on mitochondrial functions, such as inhibition of enzymatic activity [9],[51], interference with antioxidant defense [52], or the induction of the mitochondrial permeability transition [53], the idea to use this as a starting point for therapeutic approaches emerged. Mitophagy, an essential part of the mitochondrial quality control, is the selective degradation of mitochondria and relies on a functional autophagosomal and lysosomal machinery. It is therefore comprehensible that a disturbance of general autophagy might also impact mitophagy and thereby contribute in the accumulation of damaged proteins, membranes and whole organelles. Future studies are certainly needed on the mechanism of the protective role of taurine and it may be good to focus on the intricate relationship between mitochondrial function, mitophagy and autophagy in the pathogenesis of HE and potential therapies for this disease. In summary, we propose that the reported beneficial effects of taurine are at least partially caused by enhancing autophagic flux under conditions that normally would hamper autophagy. In view of these findings, we propose that promoting autophagy is a novel promising therapeutic approach in treating patients suffering from hyperammonemia. In-depth studies are necessary for evaluating the supportive therapeutic potential of taurine or similar approaches modulating autophagy in HE.

#### Declaration of Competing Interest

The authors declare to have no conflict of interest

#### CRediT authorship contribution statement

**Kaihui Lu:** Data curation, Formal analysis, Writing - original draft, Writing - review & editing. **Marcel Zimmermann:** Data curation, Formal analysis, Writing - original draft, Writing - review & editing. **Boris Görg:** Data curation, Formal analysis, Resources, Writing - review & editing. **Hans-Jürgen Bidmon:** Data curation, Formal analysis, Resources, Writing - review & editing. **Barbara Biermann:** Data curation, Formal analysis, Resources, Writing - review & editing. **Nikolaj Klöcker:** Writing - review & editing. **Dieter Häussinger:** Writing - review & editing. **Andreas S. Reichert:** Conceptualization, Project administration, Writing - original draft, Writing - review & editing.

#### Acknowledgments

The authors are grateful for tissue samples provided by the Department of Anatomy, Heinrich Heine University Düsseldorf and the New South Wales Tissue Resource Center at the University of Sydney which is supported by the [National Health and Medical Research Council](#) of Australia, Schizophrenia Research Institute, National Institute of Alcohol Abuse and Alcoholism (NIH (NIAAA) R24AA012725). The authors thank the center for advanced imaging (CAI) of the Heinrich-Heine-University Düsseldorf for the use of their equipment, Drs Helmut Sies, Peter Brenneisen, Wilhelm Stahl,

Ruchika Anand, Arun Kumar Kondadi, and Ayse Karababa for helpful discussions, Drs Niklas Berleth and Björn Stork for providing antibodies, Andrea Borhardt, Gisela Pansegrau, Torsten Janssen, Claudia Wittrock, and Julia Vedyashkin for expert technical assistance.

#### Financial support statement

Supported by the [Deutsche Forschungsgemeinschaft](#), Collaborative Research Center 974 “Communication and Systems Relevance in Liver Injury and Regeneration“, Düsseldorf (Project number 190586431), Projects A05 (DH), B04 (BG), B05 (NK) and B09 (ASR).

#### Author Contributions

KL designed and performed the majority of experiments. MZ designed and performed the experiments addressing autophagy in neurons *in vitro* and addressing the effect of taurine on autophagy signaling and ROS formation in astrocytes/astrocytoma cells. BG and HJB designed performed the *in vivo* experiments. BB designed and performed the neuron IF experiments. KL, MZ, BG, HJB, and BB performed formal data analysis and data curation. ASR, NK, DH designed experiments and obtained funding. BG, HJB, and BB provided resources. ASR developed the concept of the study and administrated the project. KL, MZ, and ASR wrote the original draft of the manuscript. All authors critically reviewed the manuscript.

#### Supplementary materials

Supplementary material associated with this article can be found, in the online version, at [doi:10.1016/j.ebiom.2019.09.058](https://doi.org/10.1016/j.ebiom.2019.09.058).

#### References

- [1] Häussinger D, Sies H. Hepatic encephalopathy: clinical aspects and pathogenetic concept. *Arch Biochem Biophys* 2013;536(2):97–100.
- [2] Parekh PJ, Balart LA. Ammonia and its role in the pathogenesis of hepatic encephalopathy. *Clin Liver Dis* 2015;19(3):529–37.
- [3] Nardone R, Taylor AC, Holler Y, Brigo F, Lochner P, Trinka E. Minimal hepatic encephalopathy: a review. *Neurosci. Res.* 2016;111:1–12.
- [4] Galland F, Negri E, Da Re C, Froes F, Strapazzon L, Guerra MC, et al. Hyperammonemia compromises glutamate metabolism and reduces BDNF in the rat hippocampus. *Neurotoxicology* 2017;62:46–55.
- [5] Suárez I, Bodega G, Fernández B. Glutamine synthetase in brain: effect of ammonia. *Neurochem. Int.* 2002;41(2):123–42.
- [6] Görg B, Qvartskhava N, Keitel V, Bidmon HJ, Selbach O, Schliess F, et al. Ammonia induces RNA oxidation in cultured astrocytes and brain *in vivo*. *Hepatology* 2008;48(2):567–79.
- [7] Schliess F, Foster N, Görg B, Reinehr R, Häussinger D. Hypoosmotic swelling increases protein tyrosine nitration in cultured rat astrocytes. *Glia* 2004;47(1):21–9.
- [8] Reinehr R, Görg B, Becker S, Qvartskhava N, Bidmon HJ, Selbach O, et al. Hypoosmotic swelling and ammonia increase oxidative stress by NADPH oxidase in cultured astrocytes and vital brain slices. *Glia* 2007;55(7):758–71.
- [9] Niknahad H, Jamshidzadeh A, Heidari R, Zarei M, Ommati MM. Ammonia-induced mitochondrial dysfunction and energy metabolism disturbances in isolated brain and liver mitochondria, and the effect of taurine administration: relevance to hepatic encephalopathy treatment. *Clin Exp Hepatol* 2017;3(3):141–51.
- [10] Rama Rao KV, Norenberg MD. Brain energy metabolism and mitochondrial dysfunction in acute and chronic hepatic encephalopathy. *Neurochem. Int.* 2012;60(7):697–706.
- [11] Haack N, Dublin P, Rose CR. Dysbalance of astrocyte calcium under hyperammonemic conditions. *PLoS ONE* 2014;9(8):e105832.
- [12] Karababa A, Görg B, Schliess F, Häussinger D. O-GlcNAcylation as a novel ammonia-induced posttranslational protein modification in cultured rat astrocytes. *Metab Brain Dis* 2014;29(4):975–82.
- [13] Oenarto J, Karababa A, Castoldi M, Bidmon HJ, Görg B, Häussinger D. Ammonia-induced miRNA expression changes in cultured rat astrocytes. *Sci Rep* 2016;6(1):18493.
- [14] Okamoto K. Organellophagy: eliminating cellular building blocks via selective autophagy. *J Cell Biol* 2014;205(4):435–45.
- [15] Yang Z, Klionsky DJ. Mammalian autophagy: core molecular machinery and signaling regulation. *Curr Opin Cell Biol* 2010;22(2):124–31.
- [16] Nunnari J, Suomalainen A. Mitochondria: in sickness and in health. *Cell* 2012;148(6):1145–59.

- [17] Czaja MJ, Ding WX, Donohue TM Jr, Friedman SL, Kim JS, Komatsu M, et al. Functions of autophagy in normal and diseased liver. *Autophagy* 2013;9(8):1131–58.
- [18] Lee S, Kim JS. Mitophagy: therapeutic potentials for liver disease and beyond. *Toxicol Res* 2014;30(4):243–50.
- [19] Soria LR, Allegri G, Melch D, Pastore N, Annunziata P, Paris D, et al. Enhancement of hepatic autophagy increases ureagenesis and protects against hyperammonemia. *Proc Natl Acad Sci U.S.A.* 2018;115(2):391–6.
- [20] Qiu J, Tsien C, Thapalaya S, Narayanan A, Wehl CC, Ching JK, et al. Hyperammonemia-mediated autophagy in skeletal muscle contributes to sarcopenia of cirrhosis. *Am J Phys Endocrinol Metab* 2012;303(8):E983–93.
- [21] Amenta JS, Hlivko TJ, McBee AG, Shinozuka H, Brocher S. Specific inhibition by NH<sub>4</sub>Cl of autophagy-associated proteolysis in cultured fibroblasts. *Exp Cell Res* 1978;115(2):357–66.
- [22] Polletta L, Vernucci E, Carnevale I, Arcangeli T, Rotili D, Palmerio S, et al. SIRT5 regulation of ammonia-induced autophagy and mitophagy. *Autophagy* 2015;11(2):253–70.
- [23] Matthiessen HP, Schmalenbach C, Müller HW. Astroglia-released neurite growth-inducing activity for embryonic hippocampal neurons is associated with laminin bound in a sulfated complex and free fibronectin. *Glia* 1989;2(3):177–88.
- [24] Kaech S, Banker G. Culturing hippocampal neurons. *Nat Protoc* 2006;1(5):2406–15.
- [25] Schroeter A, Wen S, Molders A, Erlenhardt N, Stein V, Klöcker N. Depletion of the AMPAR reserve pool impairs synaptic plasticity in a model of hepatic encephalopathy. *Mol Cell Neurosci* 2015;68:331–9.
- [26] Warskulat U, Görg B, Bidmon HJ, Müller HW, Schliess F, Häussinger D. Ammonia-induced heme oxygenase-1 expression in cultured rat astrocytes and rat brain *in vivo*. *Glia* 2002;40(3):324–36.
- [27] Anand R, Streckler V, Urbach J, Wittig I, Reichert AS. Mic13 is essential for formation of crista junctions in mammalian cells. *PLoS ONE* 2016;11(8):e0160258.
- [28] Biermann B, Ivankova-Susankova K, Bradaia A, Abdel Aziz S, Besseyrias V, Kapfhammer JP, et al. The Sushi domains of GABAB receptors function as axonal targeting signals. *J Neurosci* 2010;30(4):1385–94.
- [29] Görg B, Bidmon HJ, Häussinger D. Gene expression profiling in the cerebral cortex of patients with cirrhosis with and without hepatic encephalopathy. *Hepatology* 2013;57(6):2436–47.
- [30] Sobczyk K, Jordens MS, Karababa A, Görg B, Häussinger D. Ephrin/Ephrin receptor expression in ammonia-treated rat astrocytes and in human cerebral cortex in hepatic encephalopathy. *Neurochem Res* 2015;40(2):274–83.
- [31] Görg B, Karababa A, Shafiqullina A, Bidmon HJ, Häussinger D. Ammonia-induced senescence in cultured rat astrocytes and in human cerebral cortex in hepatic encephalopathy. *Glia* 2015;63(1):37–50.
- [32] Swain M, Butterworth RF, Blei AT. Ammonia and related amino acids in the pathogenesis of brain edema in acute ischemic liver failure in rats. *Hepatology* 1992;15(3):449–53.
- [33] Li Z, Ji X, Wang W, Liu J, Liang X, Wu H, et al. Ammonia induces autophagy through dopamine receptor D3 and MTOR. *PLoS ONE* 2016;11(4):e0153526.
- [34] Trudeau KM, Colby AH, Zeng J, Las G, Feng JH, Grinstaff MW, et al. Lysosome acidification by photoactivated nanoparticles restores autophagy under lipotoxicity. *J Cell Biol* 2016;214(1):25–34.
- [35] Yeo SY, Itahana Y, Guo AK, Han R, Iwamoto K, Nguyen HT, et al. Transglutaminase 2 contributes to a TP53-induced autophagy program to prevent oncogenic transformation. *Elife* 2016;5:e07101.
- [36] Luciani A, Vilella VR, Esposito S, Brunetti-Pierri N, Medina D, Settembre C, et al. Defective CFTR induces aggressive formation and lung inflammation in cystic fibrosis through ROS-mediated autophagy inhibition. *Nat Cell Biol* 2010;12(9):863–75.
- [37] Heidari R, Jamshidzadeh A, Ghanbarinejad V, Ommati MM, Niknahad H. Taurine supplementation abates cirrhosis-associated locomotor dysfunction. *Clin Exper Hepatol* 2018;4(2):72–82.
- [38] Heidari R, Jamshidzadeh A, Niknahad H, Mardani E, Ommati MM, Azarpira N, et al. Effect of taurine on chronic and acute liver injury: focus on blood and brain ammonia. *Toxicol Rep* 2016;3:870–9.
- [39] Bartolic M, Vovk A, Suput D. Effects of NH<sub>4</sub>Cl application and removal on astrocytes and endothelial cells. *Cell Mol Biol Lett* 2016;21:13.
- [40] Schliess F, Görg B, Fischer R, Desjardins P, Bidmon HJ, Herrmann A, et al. Ammonia induces MK-801-sensitive nitration and phosphorylation of protein tyrosine residues in rat astrocytes. *FASEB J Off Public Federa Am Soc Exper Biol* 2002;16(7):739–41.
- [41] Scherz-Shouval R, Elazar Z. Regulation of autophagy by ROS: physiology and pathology. *Trends Biochem Sci* 2011;36(1):30–8.
- [42] Scherz-Shouval R, Shvets E, Fass E, Shorer H, Gil L, Elazar Z. Reactive oxygen species are essential for autophagy and specifically regulate the activity of Atg4. *EMBO J* 2007;26(7):1749–60.
- [43] Battaglia G, Farrace MG, Mastroberardino PG, Viti I, Fimia GM, Van Beeumen J, et al. Transglutaminase 2 ablation leads to defective function of mitochondrial respiratory complex I affecting neuronal vulnerability in experimental models of extrapyramidal disorders. *J Neurochem* 2007;100(1):36–49.
- [44] Panicker KS, Jayakumar AR, Rao KV, Norenberg MD. Ammonia-induced activation of p53 in cultured astrocytes: role in cell swelling and glutamate uptake. *Neurochem Int* 2009;55(1–3):98–105.
- [45] Yin Z, Pascual C, Klionsky DJ. Autophagy: machinery and regulation. *Microb Cell* 2016;3(12):588–96.
- [46] Wang B, Abraham N, Gao G, Yang Q. Dysregulation of autophagy and mitochondrial function in Parkinson's disease. *Transl Neurodegener* 2016;5:19.
- [47] Saito M, Hirano H, Yano Y, Momose K, Yoshida M, Azuma T. Serum level of taurine would be associated with the amelioration of minimal hepatic encephalopathy in cirrhotic patients. *Hepatol Res* 2016;46(2):215–24.
- [48] Hansen SH, Andersen ML, Cornett C, Gradinaru R, Grunnet N. A role for taurine in mitochondrial function. *J Biomed Sci* 2010;17(Suppl 1):S23.
- [49] El Idrissi A. Taurine increases mitochondrial buffering of calcium: role in neuroprotection. *Amino Acids* 2008;34(2):321–8.
- [50] Jamshidzadeh A, Heidari R, Abasvali M, Zarei M, Ommati MM, Abdoli N, et al. Taurine treatment preserves brain and liver mitochondrial function in a rat model of fulminant hepatic failure and hyperammonemia. *Biomed Pharmacother* 2017;86:514–20.
- [51] Lai JC, Cooper AJ. Neurotoxicity of ammonia and fatty acids: differential inhibition of mitochondrial dehydrogenases by ammonia and fatty acyl coenzyme a derivatives. *Neurochem Res* 1991;16(7):795–803.
- [52] Kosenko E, Kaminsky Y, Kaminsky A, Valencia M, Lee L, Hermenegildo C, et al. Superoxide production and antioxidant enzymes in ammonia intoxication in rats. *Free Radic Res* 1997;27(6):637–44.
- [53] Bai G, Rama Rao KV, Murthy CR, Panicker KS, Jayakumar AR, Norenberg MD. Ammonia induces the mitochondrial permeability transition in primary cultures of rat astrocytes. *J Neurosci Res* 2001;66(5):981–91.